Wideband Multi-Carrier CDMA

Load-Adaptive MUI/ISI-Resilient Generalized Multi-Carrier CDMA with Linear and DF Receivers

GEORGIOS B. GIANNAKIS, ANASTASIOS STAMOULIS, ZHENGDAO WANG, PAUL A. ANGHEL
Dept. of Electrical and Computer Engineering, 200 Union Street S.E.
University of Minnesota, Minneapolis, MN 55455, USA
{*georgios,stamouli,zhengdao,anghel*}*@ece.umn.edu*

May 17, 2000

Abstract. A plethora of single-carrier and multi-carrier (MC) CDMA systems have been proposed recently to mitigate intersymbol interference (ISI) and eliminate multiuser interference (MUI). We present a unifying all-digital Generalized Multicarrier CDMA framework which enables us to describe existing CDMA schemes and to highlight thorny problems associated with them. To improve the bit error rate (BER) performance of existing schemes, we design block FIR transmitters and decision feedback (DF) receivers based on an inner-code/outer-code principle, which guarantees MUI/ISI-elimination regardless of the frequency-selective physical channel. The flexibility of our framework allows further BER enhancements by taking into account the load in the system (number of active users), while blind channel estimation results in bandwidth savings. Simulations illustrate the superiority of our framework over competing MC CDMA alternatives especially in the presence of uplink multipath channels.

1 INTRODUCTION

The ultimate goal in wireless CDMA systems is to support as many mobile users and as high data rates as possible given bandwidth and power constraints. Both the maximum number of mobile users that the system can support and the maximum achievable throughput depend critically upon the bit error rate (BER) performance at the physical layer. The BER performance is directly related to the ability of recovering the transmitted symbols at the receiver. Symbol recovery is mainly impeded by two factors: first, multiuser interference (MUI) and second, intersymbol interference (ISI) caused by frequency selective channels. A plethora of single-carrier and multi-carrier (MC) CDMA systems have been proposed recently to mitigate or eliminate these two factors. However, as we explain later on, no existing scheme guarantees symbol recovery in the uplink with uncoded transmissions and without imposing constraints on the multipath channel nulls. This is exactly where we start from to develop a transmission–reception framework capable of delivering superior BER performance. While making efficient use of the available bandwidth, our scheme guarantees symbol recovery regardless of the possibly unknown FIR channel by achieving deterministic MUI elimination and ISI suppression.

In the downlink, orthogonal division multiple access (OFDMA) is capable of complete MUI elimination, provided that a sufficiently long cyclic prefix is used at the transmitter. To combat frequency–selective fading, OFDMA employs frequency hopping and/or channel coding [13, pp. 213–215,220]. As a result, robustness to multipath comes at the price of increased complexity at the receiver and reduced bandwidth efficiency. On the other hand, the ability of direct sequence (DS) CDMA to exploit multipath diversity (via RAKE reception) is well documented. Capitalizing on both OFDMA's resilience to MUI and DS-CDMA's robustness against time-dispersiveness, multicarrier (MC) CDMA systems have been proposed to suppress both MUI and ISI [1, 2, 4, 9, 11, 20, 25]. In the uplink, the use of channel coding, in the form of repetition or convolutional codes, results in further BER improvements at the expense of complexity and bandwidth overexpansion [10, 14].

However, without channel coding, symbol interleaving or assumptions on the channel nulls, there is no existing scheme guaranteeing symbol recovery with FIR linear or decision-feedback (DF) receivers. In order to study the fundamental shortcomings of existing schemes, herein we develop a generalized multi-carrier (GMC) CDMA framework, capable of modeling existing MC-CDMA schemes.

Revealing thorny limitations of existing schemes is but one of the provisions of our all-digital GMC-CDMA

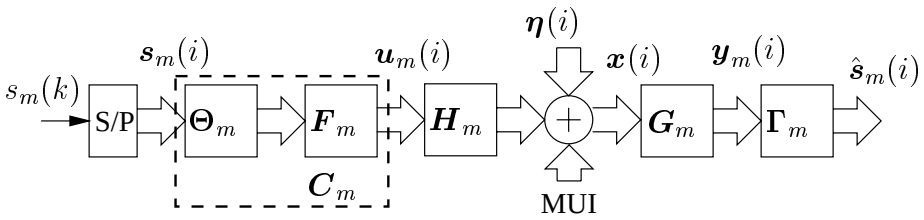

Figure 1: Discrete-time equivalent baseband transceiver model of the mth user

framework. Most importantly, our GMC-CDMA framework offers guidelines for the design of user codes in order to provide symbol recovery guarantees. To this extent, we design block FIR filterbank transmitters and linear or DF receivers based on an inner-code/outer-code principle, which guarantees MUI/ISI-resilience regardless of the frequency-selective physical channel. Unlike the MLSE receivers of [10], our multiuser DF receivers have linear complexity; they can be easily implemented either using filterbanks (in hardware) or matrix operations on a DSP chip (in software). Moreover, the flexibility of our code assignment procedure allows further BER enhancements by taking into account the load (i.e., the number of active users) in the system. Unlike existing schemes, where the code assignment does not adapt to the number of active users in the system, we show that without demanding extra transmitted power, active users in a cell can take advantage of the departure or silence of other (perhaps roaming) users by properly re-adjusting their codes. Furthermore, in wireless multimedia networks the load-adaptability of our framework can certainly benefit best-effort or constant-bit rate sessions by possibly exploiting the fluctuations of variable-bit rate sessions. Finally, dispensing with bandwidth-consuming training sequences increases the effective data transmission rate; this is made possible by our novel blind channel estimation algorithm which is tailor-made and suited to our inner-code/outer-code design.

Our load-adaptive MUI/ISI-resilient GMC-CDMA framework follows the principles of the so-called AMOUR system of [7, 22, 24], whereas the development of our multiuser DF receivers borrows from [19]. However, [7,22,24] assume a fully loaded system, and address blind channel estimation for a specific class of user codes. Herein we shed light on the load-adaptive capabilities of our framework, and we also study the role of different precoders and their impact on BER. Moreover, we show that, for the same amount of induced redundancy, our inner-code design exhibits better BER performance than BCH codes with the same decoding delays. On the other hand, [19] refers to a single-user block transmission system.

In Section 2 we develop our GMC-CDMA framework, which allows us to describe existing MC-CDMA systems in Section 3 and identify their inherent limitations. Thus, we are motivated to pursue our MUI/ISI-resilient inner-code/outer-code design in Section 4, and in Section 5 we study how the framework is modified in the case of underloaded systems. In Section 6 we show how symbol recovery can be accomplished using multiuser DF receivers and in Section 7, we derive our blind estimation algorithm. Finally, in Section 8 we illustrate the BER superiority of our designs over existing MC-CDMA schemes using extensive simulations, and give pointers for future research in Section 9.

2 System Model

First, we present a high level view and then we explain the knots and bolts of our system model. Fig. 1 depicts the all-digital baseband equivalent transmitter and receiver model for the mth user. User m uses an assigned code matrix $\mathbf{C}_m = \mathbf{F}_m\mathbf{\Theta}_m$ to transmit blocks $\mathbf{s}_m(i)$ of size K. Through the code $\mathbf{C}_m$, the $K \times 1$ vector $\mathbf{s}_m(i)$ is mapped to a $P \times 1$ vector $\mathbf{u}_m(i) = \mathbf{C}_m\mathbf{s}_m(i)$ which is transmitted over the channel. The channel, which is assumed to have finite impulse response (FIR) during the transmission of the block, is represented by the Toeplitz (convolution) matrix $\mathbf{H}_m$. The received block $\mathbf{x}(i)$ contains multiuser interference (MUI) and additive noise $\boldsymbol{\eta}(i)$. The receiver removes MUI using the filterbank described by the matrix $\mathbf{G}_m$, and retrieves the transmitted block either using the filterbank $\mathbf{\Gamma}_m$ or a DF receiver described by the matrices $\mathbf{W}_m$ and $\mathbf{B}_m$ (see Fig. 2).

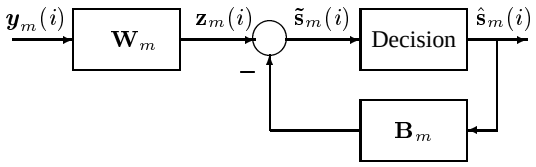

Figure 2: GMC-CDMA DF receiver of the mth user

In more detail, signals, codes, and channels of the uplink CDMA are represented by samples of their complex envelopes taken at the chip rate. The data symbol sequence of the m-th user is denoted by $s_m(k)$ and through serial-to-parallel converters is grouped into blocks of K symbols $\mathbf{s}_m(i) := [s_m(iK) \dots s_m(iK+K-1)]^T$. Using the order $P-1$ FIR precoding filterbank $\{c_{m,k}(n)\}_{k=0}^{K-1}$, the

block $\mathbf{s}_m(i)$ is mapped to a block $\mathbf{u}_m(i)$ of $P > K$ chips: $\mathbf{u}_m(i) = \mathbf{C}_m\mathbf{s}_m(i)$, where the (n,k)th entry of the $P \times K$ matrix $\mathbf{C}_m$ is $c_{m,k}(n)$. The mapping of K input symbols to P output chips is conceptually performed in two phases: first, the *inner code* is applied to facilitate ISI suppression, and, second, the *outer code* is applied to accomplish MUI elimination. The inner code is represented by the $J \times K$ matrix $\mathbf{\Theta}_m$, whereas the outer code is represented by the $P \times J$ matrix $\mathbf{F}_m$ ($P \geq J \geq K$). The intuition behind the factoring of the code matrix $\mathbf{C}_m$ into $\mathbf{\Theta}_m$ and $\mathbf{F}_m$ is that MC-CDMA systems introduce redundancy to combat ISI and MUI; ISI-related redundancy can be built-in using $\mathbf{\Theta}_m$, whereas MUI-related redundancy can be introduced using $\mathbf{F}_m$. Though $\mathbf{C}_m$ is not capable of modeling all possible forms of channel coding, error-control codes are not precluded from our GMC-CDMA system. A possible channel encoder should precede the block-spreading operation that $\mathbf{C}_m$ implements, and either operate before the S/P converter (e.g., as in the case of a convolutional code) or after the S/P converter (e.g., as in the case of a Reed-Solomon code).

The coded chip sequence $u_m(n)$ passes through the discrete-time equivalent baseband channel $h_m(n)$, which is assumed to be of order $\leq L$ (a common assumption in quasi-synchronous CDMA systems [7]). The impulse response $h_m(n)$ models multipath, transmit-receive filters, and the mth user's asynchronism in the form of delay factors [7]. The chip-sampled sequence is: $x(n) = \sum_{m=0}^{M-1} x_m(n) + \eta(n)$, where: $x_m(n) = \sum_{j=0}^{L} h_m(j)u_m(n-j)$, and $\eta(n)$ is the additive noise. To avoid channel-induced inter-block interference (IBI), we design our transmitted blocks $\mathbf{u}_m(n)$ to have L trailing zeros (TZ), which act as "guard bits": in our matrix formulation, the lower $L \times J$ submatrix of $\mathbf{F}_m$ is set to an all-zero $L \times J$ matrix $\mathbf{0}_{L\times J}$. As detailed in [22, 24], the trailing zeros at the transmitter can be replaced by a cyclic prefix (CP) that similar to OFDM must be discarded at the receiver to eliminate IBI. With TZ transmissions, the received $P \times 1$ vector $\mathbf{x}(i) := [x(iP) \ldots x(iP+P-1)]^T$ in AGN $\boldsymbol{\eta}(i) := [\eta(iP) \ldots \eta(iP+P-1)]^T$ can be expressed as:

$$\mathbf{x}(i) = \sum_{m=0}^{M-1} \mathbf{H}_m\mathbf{C}_m\mathbf{s}_m(i) + \boldsymbol{\eta}(i)\,, \qquad (1)$$

where $\mathbf{H}_m$ is a $P \times P$ Toeplitz (convolution) matrix with (i,j) entry $h_m(i-j)$.

At the receiver end, recovery of the transmitted block $\mathbf{s}_m(i)$ entails two actions: i)elimination of MUI, and ii)elimination of multipath induced ISI (within a block). These actions are implemented by filterbanks performing block processing that amounts to multiplying blocks by the matrices $\mathbf{G}_m$, $\mathbf{W}_m$, and $\mathbf{B}_m$. The first stage of the receiver for user m consists of J parallel filters $\{g_{m,j}(p)\}_{j=0}^{J-1}$, each of length P. The taps of the filters are given by the entries of the $J \times P$ matrix $\mathbf{G}_m$ with (j,p) entry $[\mathbf{G}_m]_{j,p} = g_{m,j}(p)$. The matrix $\mathbf{G}_m$ maps the block $\mathbf{x}(i)$ to an MUI-free block $\mathbf{y}_m(i)$:

$$\mathbf{y}_m(i) = \mathbf{G}_m\mathbf{H}_m\mathbf{C}_m\mathbf{s}_m(i) + \mathbf{G}_m\boldsymbol{\eta}(i) + \underbrace{\sum_{\mu=0,\mu\neq m}^{M-1} \mathbf{G}_m\mathbf{H}_\mu\mathbf{C}_\mu\mathbf{s}_\mu(i)}_{\text{MUI}}\,. \qquad (2)$$

We can deduce from (2), that the precoder $\mathbf{C}_m$ and the receiver $\mathbf{G}_m$ should be designed in such a way that MUI is made as small as possible. In Section 4 we provide a joint design procedure for the receiver $\mathbf{G}_m$ and the outer code $\mathbf{F}_m$ which leads to MUI elimination regardless of the physical channel. We will also see how the proper choice of the inner code $\mathbf{\Theta}_m$ guarantees the ISI removal and symbol recovery from the MUI-free block $\mathbf{y}_m(n)$. But first, we motivate the importance of our design procedure by looking at existing multiuser multicarrier CDMA systems (see [6] for detailed derivations of all-digital equivalent models).

3 EXISTING MC-CDMA SYSTEMS

In this section we explore how our GMC-CDMA framework enables us to identify fundamental shortcomings of existing schemes. First we see how various CDMA systems can be modeled using the results of Section 2, and then we show why existing schemes cannot guarantee symbol recovery regardless of the physical channel.

3.1. SC-DS-CDMA: The simplest of the CDMA transmission systems uses a single carrier (SC) and each symbol is spread by a code $\mathbf{c}_{\mu,0} = [c_\mu(0) \ldots c_\mu(P-1)]^T$ of processing gain P. It follows that a SC-DS-CDMA system can be modeled in our framework by setting $\mathbf{C}_\mu := \mathbf{c}_{\mu,0}$; thus, the $P \times K$ code matrix $\mathbf{C}_\mu$ in (1) reduces to a $P \times 1$ vector, $\mathbf{c}_{\mu,0}$, the entries of which represent the chips of a Gold, Walsh-Hadamard, or pseudo-noise (PN) ± 1 sequences. The fundamental shortcoming of SC-DS-CDMA is that there may exist channels for which the user symbols are not identifiable from the received signal. For example, suppose that we have a SC-DS-CDMA system with 2 users: user "1" with $K = 1$, $P = 4$, uses the Walsh-Hadamard code $\mathbf{c}_{1,0} = [-1\ , -1\ , 1\ , 1]^T$, and transmits the data over the channel $h_1(n) = \delta(n) - \delta(n-1)$; user "2" uses the code $\mathbf{c}_{2,0} = [1\ , -1\ , -1\ , 1]^T$ and transmits over the channel $h_2(n) = \delta(n) + \delta(n-1)$. If user "2" is silent and user "1" transmits $s_1(n) = -\delta(n)$ (which corresponds to "-1" in BPSK), the received signal $x(n) = \delta(n) - 2\delta(n-2) + \delta(n-4)$ is identical to the case where user "1" is silent and user "2" transmits $s_2(n) = \delta(n)$ (which is "1" in BPSK). In other words, if both users transmit at the same time, it is impossible to recover at the receiver the transmitted symbols, even though the user codes are orthogonal. Therefore, spreading at the symbol level fails to guarantee symbol recovery; we will

show in Section 4 that spreading (i.e., precoding) at the *block of symbols* level will make symbol recovery possible regardless of the underlying FIR channel.

3.2. MC-CDMA: By combining spreading with multicarrier modulation, multi-carrier (MC) CDMA schemes constitute a natural extension of SC-CDMA systems (see e.g., [5] and [9]). The basic idea is that with IFFT processing at the transmitter, and FFT processing at the receiver, frequency-selective multipath channels are converted to flat fading channels; all users share the same subcarriers and MUI suppression is achieved by their linearly independent chip sequences $\mathbf{c}_{\mu,0}$. Our framework encompasses MC-CDMA systems by setting $K := 1, \forall \mu$, and $\mathbf{C}_\mu := \mathbf{c}_\mu = \mathbf{F}\mathbf{c}_{\mu,0}$, where $\mathbf{c}_{\mu,0}$ is chosen as in SC-DS-CDMA, while the $P \times P$ matrix $\mathbf{F}$ with (p_1, p_2) entry $[\mathbf{F}]_{p_1,p_2} = \exp(j2\pi p_1 p_2/P)$, $0 \leq p_1, p_2 \leq P-1$, implements the Inverse Fast Fourier Transform (IFFT) of each user's chip sequence $\mathbf{c}_{\mu,0}$ (the matrix $\mathbf{F}$ is common to all the users).

3.3. MC-DS-CDMA: Whereas in MC-CDMA systems information about a specific source symbol is transmitted on every subcarrier, in MC-DS-CDMA each subcarrier carries only a subset of the source symbols. Specifically, the source symbols $s_\mu(n)$ of every user are first S/P-converted into N_c substreams $\{s_{\mu,k}(n)\}_{k=0}^{N_c-1}$. Then, each substream is spread with a P-long DS code $\mathbf{c}_{\mu,0}$, which has spectral support $[-\alpha, \alpha]$, ($\alpha < \pi$) (the DS code is user-specific). The spread substreams $s_{\mu,k}(n)\mathbf{c}_{\mu,0}$ are then modulated on subcarriers $\{f_k\}_{k=0}^{N_c-1}$ with subcarrier spacing $\triangle f_i \leq \alpha$ [9, 16]. The primary motivation behind MC-DS-CDMA schemes is their increased bandwidth efficiency (compared to MC-CDMA), which, however, comes at the price of BER performance degradation (because of inter-carrier interference and channel nulls potentially hitting a particular subcarrier). Our filterbank model in (1) describes an MC-DS-CDMA system by choosing the $P \times K$ code matrix in (1) as $\mathbf{C}_\mu = [\mathbf{D}_p(f_1)\mathbf{c}_{\mu,0}, \ldots, \mathbf{D}_p(f_{N_c})\mathbf{c}_{\mu,0}]$, where $\mathbf{D}_p(f_i)$ is a $P \times P$ diagonal matrix with (n,n)th element equal to $\exp(j2\pi f_i n)$, $i = 0, \ldots, N_c - 1$. Unfortunately, MC-DS-CDMA suffers from the same symbol recovery problems as DS-CDMA. This is because each symbol substream $s_{\mu,k}(n)$ can be thought of as a separate DS-CDMA system which modulates the subcarrier at frequency f_k.

3.4. MT-CDMA: A special case of MC-DS-CDMA are Multi-tone (MT) CDMA systems: the subcarrier frequencies are now chosen as $f_i = i/P$ [20]. It is straightforward to see how MT-CDMA systems can be modeled using our GMC-CDMA framework (see [6] for details). □

As we have shown, the GMC-CDMA model can be used to describe several existing CDMA schemes. But none of the aforementioned models guarantees MUI/ISI-free multirate transmissions and user symbol recovery in the presence of (possibly unknown) multipath (uplink or downlink) channels without bandwidth expansion.

4 MUI/ISI ELIMINATING CODES

In this section we present our algorithm for the design of an MUI/ISI-resilient CDMA system capable of alleviating fading effects and of providing symbol recovery regardless of the (possibly unknown) FIR channels. First, we will give an intuitive description of how we go about: i)eliminating MUI in the frequency ($\mathcal{Z}$-) domain, and ii) guaranteeing symbol recovery regardless of the physical channel. Our approach lies in the fundamental mechanism of redundant spreading at the *block of symbols* level; interestingly enough, this mechanism is the natural evolution and combination of already existing techniques.

Our origin is the observation that if users transmit over different frequencies (transmitting orthogonal signals in the FDMA sense), the orthogonality between the users' signals will be preserved at the receiver. However, should a user use only one subcarrier (as in OFDMA), it would not be possible to recover the transmitted symbols at the receiver, if the user's channel happened to have a null at this particular subcarrier. Even if the subcarrier is close to a channel zero, the user's signal will be greatly attenuated, which inevitably leads to poor performance. A natural solution which guarantees identifiability of the user symbols is given by a multi-carrier approach, where each user's data are transmitted over more than one frequencies (subcarriers). Such a guarantee can be given as long as the channel has finite number (say at most L) zeros: then for symbol recovery, it suffices for every user to transmit each symbol on $L+1$ frequencies. Unfortunately, like MC-CDMA, the price paid is bandwidth over-expansion: we need L times larger bandwidth than the OFDMA system. This is exactly where the novelty of our spreading at the block-of-symbols level stems from: to overcome this bandwidth over-expansion, we transmit a group of K symbols using $K+L$ frequencies with $K \gg L$; as a direct result, the bandwidth expansion factor $(K+L)/K$ can be brought arbitrarily close to 1. Under such a transmission scheme, the challenge is in designing the code so that the K symbols can be recovered from any of the K subcarriers. By doing this, symbol recovery will also be guaranteed, as at most L of the $K+L$ subcarriers can be nullified by the channel.

To see how the aforementioned line of thought can be cast rigorously in the mathematical framework of Section 2, we assume that $N = M(K+L)$ subcarriers are available to users. We look at the practically appealing case where the N subcarriers are distributed uniformly in an allocated frequency band, and we refer to each of the $l = 0, 1, \ldots, N-1$ subcarriers using the FFT frequencies $\exp(j2\pi l/N)$. We consider the partition of the set $\boldsymbol{\mathcal{F}} = \{\exp(j2\pi l/N)\ ,\ l = 0 \ldots (N-1)\}$ into M disjoint subsets $\boldsymbol{\mathcal{F}}_m$; each subset contains the subcarriers which are allocated to user m. Then the outer code matrix $\mathbf{F}_m$ can be

built as:

$$\mathbf{F}_m = \left[\begin{array}{c} \mathbf{F}^{\mathcal{H}} \mathbf{\Phi}_m \\ \mathbf{0}_{P \times L} \end{array} \right]. \quad (3)$$

The $N \times N$ matrix $\mathbf{F}$ has entries $[\mathbf{F}]_{l,k} = \exp(-j2\pi lk/N)$, $0 \leq l \leq N-1$, $0 \leq k \leq N-1$, whereas the subcarrier-selector $N \times J$ matrix $\mathbf{\Phi}_m$ has entries $[\mathbf{\Phi}_m]_{l,k} = 1$, if $\exp(j2\pi l/N) \in \boldsymbol{\mathcal{F}}_m$, and 0 otherwise.

From an implementation point of view, the outer code $\mathbf{F}_m$ takes the IFFT of the users' data (which is computationally not expensive) and zero-pads them to obviate IBI. The matrix $\mathbf{\Phi}_m$ performs the subcarrier selection which realizes MUI elimination, as each user transmits symbols only on his/hers respective subcarriers. At the receiver end, setting $\mathbf{G}_m := \mathbf{\Phi}_m^T \mathbf{F}$ isolates the subcarriers of the user of interest, and eliminates MUI. Hence, with low (FFT-based) implementation overhead, the design of our outer code guarantees MUI elimination. Channel-irrespective symbol recovery is taken care of by proper selection of the inner code $\mathbf{\Theta}_m$ which determines the $K+L$ linear combinations of the K input symbols that are transmitted over the $K+L$ subcarriers.

As at most L of the $K+L$ subcarriers could be hit by a channel null, any K subcarriers samples at the receiver should be sufficient for symbol recovery. Hence, it suffices to design the inner code $\mathbf{\Theta}_m$ such that any K rows are linearly independent. In this work we look at the following alternatives for $\mathbf{\Theta}_m$:

Vandermonde Spreading (Va-S): $\mathbf{\Theta}_m$ is a $J \times K$ Vandermonde matrix with entries $[\mathbf{\Theta}_m]_{j,k} = \rho_{m,j}^{-k}$, $0 \leq j \leq J-1$, $0 \leq k \leq K-1$. The complex constants $\rho_{m,j}$'s are chosen to be distinct, i.e, $\rho_{m,j_1} \neq \rho_{m,j_2}$, for $j_1 \neq j_2$, to guarantee the full column rank property of $\mathbf{\Theta}_m$. In [7], the complex constants $\{\rho_{m,j}\}_{j=0}^{J-1}$ are termed "signature points" for user m, and when chosen equispaced on the unit circle, it can be shown that $\mathbf{\Theta}_m$ becomes a truncated FFT matrix.

Walsh Hadamard Spreading (WH-S): $\mathbf{\Theta}_m$ is set equal to a truncated $J \times K$ Walsh-Hadamard (WH) matrix.

Pseudo-Noise Spreading (PN-S): $\mathbf{\Theta}_m$ is set equal to a random $J \times K$ matrix with equiprobable $\pm 1, \pm j$ entries.

As a result, our inner-code/outer-code design guarantees:

$$\begin{array}{rcl} \mathbf{G}_m \mathbf{H}_\mu \mathbf{C}_\mu & = & \mathbf{0}_{J \times K}\ ,\ \forall \mu \neq m \\ \mathbf{G}_m \mathbf{H}_m \mathbf{C}_m & & \text{has full rank}\ ,\ \forall m\ , \end{array} \quad (4)$$

which are the requirements for MUI/ISI elimination (c.f. (2)). The resulting MUI-free block $\mathbf{y}_m(i)$ is given by:

$$\mathbf{y}_m(i) = \mathbf{D}_{H_m} \mathbf{\Theta}_m \mathbf{s}_m(i) + \mathbf{G}_m \boldsymbol{\eta}(i)\ , \quad (5)$$

where

$\mathbf{D}_{H_m} := \mathrm{diag}\big(H_m(e^{j\frac{2\pi}{N} l_{m,0}}), \ldots, H_m(e^{j\frac{2\pi}{N} l_{m,(J-1)}})\big)$

is a diagonal matrix comprised of the frequency response of the mth users' channel at the respective allocated subcarriers. The transmitted symbols $\mathbf{s}_m(i)$ can be retrieved from $\mathbf{y}_m(i)$ using a linear receiver $\mathbf{\Gamma}_m$. From (5) we observe that the outer code rendered the multi-user system equivalent to M single users. As a result, the linear receiver is given by [15]: $\mathbf{\Gamma}_m^{\mathrm{zf}} = (\mathbf{D}_{H_m} \mathbf{\Theta}_m)^\dagger$ for a zero-forcing linear receiver. In Section 6 we will see that a DF receiver results in improved BER performance.

At the price of increased implementation overhead, general frequencies on the $\mathcal{Z}$-plane (instead of frequencies on the unit circle used here and in [24]) can be used to carry the users' symbols, which is basically the approach taken in [7]. At this point, we underline that though the design of the outer code is reminiscent of FDMA, there are distinct features which make the GMC-CDMA approach superior. First, our solution is based on an all-digital implementation which dispenses with FDMA-induced analog implementation problems such as subchannel leakage and inflexibility in subcarrier allocation (in our scheme, subcarrier allocation amounts to properly setting the entries of $\mathbf{\Phi}_m$). Second, our novel design of the inner code guarantees symbol recovery even when CSI is not available at the transmitter as long as there is an upper bound on the channel order. In cellular networks the channel is time-varying but an upper bound on the channel order is available (based on previous measurements). Hence, unlike existing work on multi-user DMT (see, e.g., [3]) which requires CSI at the transmitter, our work has a significant practical appeal in wireless environments. The latter include cellular and ad hoc (Bluetooth [8]-like) networking if frequency-hopping is introduced via $\mathbf{\Phi}_m$ along the lines of [26].

We remark that our code design is amenable to optimization when CSI is available at the transmitter. At the user level, following a "water-filling" principle, the inner code $\mathbf{\Theta}_m$ could be optimized to maximize the mutual information rate. The optimization of the outer code is at the system level, where the allocation of subcarriers could take into account the deep fades of the users' channels (i.e., a subcarrier close to a user's channel null should not be allocated to this specific user). Both optimizations delineate future research avenues along the lines of our previous work on single-user block transmission systems.

We summarize the inner-code/outer-code design procedure in the following algorithm:

Global Design Decisions

- Given allocated frequency band, decide on the number of subcarriers N (a power of two).
- Given an upper bound on the channel order, and the number of users select K and M.
- Partition the set $\boldsymbol{\mathcal{F}}$ of available subcarriers to M disjoint sets $\boldsymbol{\mathcal{F}}_m$.

Transmitter Design for User m

- Define the outer code $\mathbf{F}_m$ using the subcarrier allocation as described by $\boldsymbol{\mathcal{F}}_m$ and (3).
- Select the inner code matrix $\mathbf{\Theta}_m$ such that any K rows

of $\mathbf{\Theta}_m$ are linearly independent[1].
• Transmit the spread sequence $\mathbf{u}_m(i) = \mathbf{F}_m \mathbf{\Theta}_m \mathbf{s}_m(i)$.

Receiver Design for User μ
• Apply the matrix $\mathbf{G}_\mu = \mathbf{\Phi}_m^T \mathbf{F}$ to the received data $\mathbf{x}(i)$ to obtain the MUI free data:

$$\mathbf{y}_\mu(i) = \mathbf{D}_{H_\mu} \mathbf{\Theta}_\mu \mathbf{s}_\mu(i) + \mathbf{G}_\mu \mathbf{w}(i)\,,$$

• Use a linear receiver as in [7,22,24] or the DF receiver of Section 6 to recover the transmitted data.

5 UNDERLOADED SYSTEMS

When the number of active users in the system decreases, the "extra bandwidth" can be utilized by the remaining users either to increase their transmission rates or to improve their BER. In our framework, the extra bandwidth manifests itself as unutilized subcarriers, which are distributed to the active users. If we recall that $K = J - L$ is the number of transmitted symbols in every transmission round, then the allocation of extra subcarriers to a user (which increases J) effectively increases the data transmission rate (as K is also increased). Starting from a partition of the set $\mathcal{F}$ of available subcarriers to M disjoint sets $\mathcal{F}_m$ (where it is no longer required that their cardinalities $|\mathcal{F}_{m_1}| = |\mathcal{F}_{m_2}|$, $\forall m_1 \neq m_2$), user m relies on $J_m = |\mathcal{F}_m|$ allocated subcarriers to transmit $K_m = J_m - L$ information symbols in each transmission round. The outer code $\mathbf{F}_m$ is $P \times J_m$, and the inner code $\mathbf{\Theta}_m$ is $J_m \times K_m$; as K_m determines the effective transmission rate of user m, our framework supports multirate services at the physical layer (see also [10, 17, 22–24]).

Multirate capabilities at the physical layer can be exploited by a properly designed wireless network framework. As illustrated in [17], in a wireless network the provision of QoS in terms of delay and throughput depends critically upon the interaction of the network layer, the medium access control (MAC), and the physical layer. The scheduler, which operates at the network layer, determines the transmission order of packets, and as a result, the transmission rate of mobile users. Through a demand-assignment MAC, the transmission rates are communicated between the base station and the mobile users. The cardinalities of the subsets $\mathcal{F}_m$ are set proportional to the allocated transmission rates, and the transmit/receive filterbanks are modified accordingly. The key in the integration between the network/MAC/physical layers is our code assignment procedure which guarantees transmission rates of arbitrarily fine resolution [17, 23].

The approach of [17, 23] has the downside that more transmitted power is required, as more data symbols are sent during the transmission round. Herein we use the extra subcarriers to improve the BER while keeping both the data transmission rate and the transmitted power constant. Such an approach is not only useful in cases where there are very tight constraints on battery life (e.g., in handsets), but it is also useful in constant-bit rate (CBR) applications (e.g., voice).

From a practical point of view, when the number of active users is M_a, $\mathcal{F}$ is partitioned to M_a subsets $\mathcal{F}_m^{(a)}$, $1 \leq m \leq M_a$, and each active user is allocated $J_a = |\mathcal{F}_m^{(a)}| = \lfloor JM/M_a \rfloor$ subcarriers. The increased spreading of K input symbols in realized by the enlarged inner-code matrix $\mathbf{\Theta}_m^{(a)}$ which is $J_a \times K$. As a result, transmit diversity is increased without any impact on transmission rate, power per user, and system-wide bandwidth. As we illustrate in the Simulations section, the increase of transmit subcarriers from J to J_a results in improved BER.

6 DF RECEIVERS

As we saw in Section 4, our MUI eliminating codes render the multi-user channel equivalent to M_a independent single-user channels. As (5) suggests, the recovery of the users' transmitted symbols amounts to inverting the channel matrix $\mathbf{H}_m$ using a zero-forcing matrix inverse or an MMSE-receiver matrix ("Wiener inverse"). Indeed, at high signal-to-noise ratios (SNR), a linear ZF equalizer structure is expected to equalize the channel perfectly. However, BER performance can be improved (especially at low SNR) in two ways. First, by exploiting the finite alphabet of the input and taking into account decisions about the symbols in the same block. Second, by whitening the noise at the input of the decision device. Noise whitening makes symbol-by-symbol detection optimal; thus, symbol-by-symbol detection is desirable from a practical point of view. Therefore, the question which naturally arises is whether there exists a linear receiver capable of making the noise samples independent at the input of the decision device. In single-user block transmission systems, if CSI is available at the transmitter, then joint design of the linear transmit/receive filterbanks (as a function of the channel and the noise autocorrelation) assures symbol recovery with white noise at the input of the decision device [15]. These results could be readily applied to our multiuser framework because the outer code transforms the multiuser channel to a single-user channel. Unfortunately, CSI is required at the transmitter. Fortunately, with a DF receiver, CSI is not required at the transmitter. Hence, both noise whitening and exploitation of finite alphabet/past decisions can be realized through our block zero-forcing (ZF) DF that we develop next.

Figure 2 depicts the structure of the DF receiver. The decision feedback equalizer consists of the feedforward filterbank represented by the $K \times J$ matrix $\mathbf{W}_m$, the decision device and the feedback filterbank represented by the $K \times K$ matrix $\mathbf{B}_m$. The feedforward filter is responsible for eliminating ISI from "future" symbols within the current block, whereas the feedback filter is responsible for

[1]The results of the Simulations section could serve as road-map to select among possible alternatives.

eliminating ISI from "past" symbols.

Let us define the $K \times 1$ vectors: $\mathbf{z}_m(i) := [\, z_m(iK)\ z_m(iK+1)\ \ldots\ z_m(iK+K-1)\,]^T$, and $\tilde{\mathbf{s}}_m(i) := [\, \tilde{s}_m(iM)\ \tilde{s}_m(iK+1)\ \ldots\ \tilde{s}_m(iK+K-1)\,]^T$. Based on (5) we obtain:

$$\mathbf{z}_m(i) = \mathbf{W}_m\mathbf{D}_{H_m}\mathbf{\Theta}_m\mathbf{s}_m(i) + \mathbf{W}_m\mathbf{G}_m\boldsymbol{\eta}(i) \quad (6a)$$

$$\tilde{\mathbf{s}}_m(i) = \mathbf{z}_m(i) - \mathbf{B}_m\hat{\mathbf{s}}_m(i) \quad (6b)$$

$$\hat{\mathbf{s}}_m(i) = Q(\tilde{\mathbf{s}}_m(i)) \quad (6c)$$

where $Q(\cdot)$ is the quantizer used by the decision device.

Symbol-by-symbol detection is rendered optimal by allowance for "successive cancellation", and whitening of the noise at the input of the decision device. Additionally, the ZF-DFE receiver should guarantee zero-forcing: in the absence of noise and under the assumption of correct past decisions, the decision statistic should be equal to the transmitted data: $\tilde{\mathbf{s}}_m(i) = \mathbf{s}_m(i) = \hat{\mathbf{s}}_m(i)$. In view of (6), the latter translates the ZF requirement to:

$$\mathbf{W}_m\mathbf{D}_{H_m}\mathbf{\Theta}_m = \mathbf{B}_m + \mathbf{I}_K.$$

Because past decisions are assumed correct, the noise at the input of the decision device is $\mathbf{W}_m\mathbf{G}_m\boldsymbol{\eta}(i)$, and in order to whiten it we select $\mathbf{W}_m$ such that:

$$\mathbf{W}_m\mathbf{G}_m\mathbf{G}_m^{\mathcal{H}}\mathbf{W}_m^{\mathcal{H}} = \mathbf{I}_K.$$

Finally, "successive cancellation" is made possible by selecting the feedback matrix $\mathbf{B}_m$ strictly upper triangular. By successive cancellation we mean that for every block indexed by i, the $(K-1)$st symbol is recovered first; then the estimate $\hat{s}_m(iK+K-1)$ is weighted by the last column of $\mathbf{B}_m$ and is removed from $\mathbf{z}_m(i)$ so that the remaining symbols can be recovered. The $(K-2)$nd symbol is recovered next, and the estimate $\hat{s}_m(iK+K-2)$ is removed from $\mathbf{z}_m(i)$. This procedure is carried out until all the symbols of the current block i have been estimated.

It can verified by direct substitution that the following assignment of $(\mathbf{W}_m, \mathbf{B}_m)$ satisfies the requirements for the ZF-DFE receiver:

$$\mathbf{W}_m = \mathbf{U}_m^{-\mathcal{H}}(\mathbf{V}_m^{-\mathcal{H}}\mathbf{D}_{H_m}\mathbf{\Theta}_m)^{\mathcal{H}} \quad (7a)$$

$$\mathbf{B}_m = \mathbf{U}_m - \mathbf{I}_K\,, \quad (7b)$$

where $\mathbf{V}_m$ and $\mathbf{U}_m$ are the Cholesky factors of the *strictly positive definite* matrices $\mathbf{G}_m\ \mathbf{G}_m^{\mathcal{H}}$ and $(\mathbf{V}_m^{-\mathcal{H}}\mathbf{D}_{H_m}\mathbf{\Theta}_m)^{\mathcal{H}}\ (\mathbf{V}_m^{-\mathcal{H}}\mathbf{D}_{H_m}\mathbf{\Theta}_m)$, respectively.

The latter matrices are guaranteed to be positive definite because of our inner-code/outer-code design. The feedforward and feedback matrices in (7) are reminiscent of the "whitened matched filter" DFE pair (see, e.g., [21, pg. 59]), where $\mathbf{U}^{\mathcal{H}}\mathbf{U}$ is only positive semi-definite; from a practical point of view, symbol recovery is guaranteed only if the DF matrices are full rank, which amounts to the positive definiteness of $\mathbf{U}^{\mathcal{H}}\mathbf{U}$. Our novel code design assures positive-definiteness and is precisely why it satisfies perfectly the ZF property regardless of the channel nulls with the block FIR DF settings of (7). Similar to linear Wiener receivers one could also trade-off ISI for noise suppression using an MMSE-DFE receiver whose derivation we omit due to lack of space.

7 BLIND CHANNEL ESTIMATION

In the previous sections we saw that the design requirement on the inner code $\mathbf{\Theta}_m$ (i.e., any K rows should be linearly independent) guarantees symbol recovery regardless of the channel. In this section we develop a blind channel estimation algorithm based on the properties of $\mathbf{\Theta}_m$. Similar to existing subspace-based methods, in our algorithm the channel response is estimated (within a scale) as the unique null-vector of a matrix which depends only on the received data. Unlike most existing subspace-based methods[2] our algorithm guarantees blind channel identifiability regardless of the channel nulls.

To satisfy the persistence of excitation property, the receiver collects N_b blocks $\mathbf{y}_m(i)$, $0 \le i \le N_b - 1$ and forms the matrix $\boldsymbol{\mathcal{Y}}_m := \big[\mathbf{y}_m(0)\ldots\mathbf{y}_m(N_b-1)\big]$, which corresponds to $\boldsymbol{\mathcal{S}}_m := \big[\mathbf{s}_m(0)\ldots\mathbf{s}_m(N_b-1)\big]$. If N_b is sufficiently large, then $\boldsymbol{\mathcal{S}}_m\boldsymbol{\mathcal{S}}_m^{\mathcal{H}}$ has full rank K, and in the absence of noise the matrix $\boldsymbol{\mathcal{Y}}_m\boldsymbol{\mathcal{Y}}_m^{\mathcal{H}}$, which is equal to $(\mathbf{D}_{H_m}\mathbf{\Theta}_m\mathbf{S}_m)(\mathbf{D}_{H_m}\mathbf{\Theta}_m\mathbf{S}_m)^{\mathcal{H}}$, will also have rank K. Hence, the range space $\mathcal{R}(\boldsymbol{\mathcal{Y}}_m\boldsymbol{\mathcal{Y}}^{\mathcal{H}})$ will be equal to $\mathcal{R}((\mathbf{D}_{H_m}\mathbf{\Theta}_m\mathbf{S}_m)(\mathbf{D}_{H_m}\mathbf{\Theta}_m\mathbf{S}_m)^{\mathcal{H}})$. If we consider the eigen-decomposition of $\boldsymbol{\mathcal{Y}}_m\boldsymbol{\mathcal{Y}}_m^{\mathcal{H}}$:

$$[\mathbf{U}_m\ \tilde{\mathbf{U}}_m]\begin{bmatrix}\mathbf{\Lambda}_{mK\times K} & \mathbf{0}_{K\times(J-K)}\\ \mathbf{0}_{(J-K)\times K} & \mathbf{0}_{(J-K)\times(J-K)}\end{bmatrix}\begin{bmatrix}\mathbf{U}_m^{\mathcal{H}}\\ \tilde{\mathbf{U}}_m^{\mathcal{H}}\end{bmatrix},$$

then the matrix $\tilde{\mathbf{U}}_m$ is $J\times(J-K)$, because the nullity of $\boldsymbol{\mathcal{Y}}_m\boldsymbol{\mathcal{Y}}_m^{\mathcal{H}}$ is $J-K$. Given that $\mathcal{R}(\boldsymbol{\mathcal{Y}}_m\boldsymbol{\mathcal{Y}}_m^{\mathcal{H}}) = \mathcal{R}(\mathbf{D}_{H_m}\mathbf{\Theta}_m)$, and $\tilde{\mathbf{U}}_m$ spans the null space of $\boldsymbol{\mathcal{Y}}_m\boldsymbol{\mathcal{Y}}_m^{\mathcal{H}}$, we readily obtain that for every column $\tilde{\mathbf{u}}_{m,i}$ of $\tilde{\mathbf{U}}_m$ $(0 \le i \le J-K-1)$ it holds: $\tilde{\mathbf{u}}_{m,i}^{\mathcal{H}}\mathbf{D}_{H_m}\mathbf{\Theta}_m = \mathbf{0}_{1\times K}$.

If we recall that $\mathbf{D}_{H_m}$ is diagonal, then we can "interchange" the order of $\tilde{\mathbf{u}}_{m,i}^{\mathcal{H}}$, and $\mathbf{D}_{H_m}$ (as (8) indicates), and obtain (9). From (9), we infer that:

$$\mathbf{h}_m^T\mathbf{A}_m\mathbf{D}_{u_{m,i}}\mathbf{\Theta}_m = \mathbf{0}_{1\times K},$$

and by using all $J-K$ columns of $\tilde{\mathbf{U}}_m$, we obtain:

$$\mathbf{h}_m^T\mathbf{A}_m\big[\mathbf{D}_{u_{m,0}}\mathbf{\Theta}_m\ \ldots\ \mathbf{D}_{u_{m,J-K-1}}\mathbf{\Theta}_m\big] = \mathbf{0}_{1\times K(J-K)}\,. \quad (10)$$

It can be shown that the matrix

$$\mathbf{A}_m\big[\mathbf{D}_{u_{m,0}}\mathbf{\Theta}_m\ \ldots\ \mathbf{D}_{u_{m,J-K-1}}\mathbf{\Theta}_m\big]$$

has left null-space of dimensionality one, which guarantees that, within a scale, the channel $\mathbf{h}_m$ can be identified uniquely [6].

8 SIMULATIONS

In this section we study the BER performance and we focus on four facets of our system: load-adaptability, blind

[2] One exception is our previous work for single-user block transmission systems [15].

$$\tilde{\mathbf{u}}_{m,i}^{\mathcal{H}}\mathbf{D}_{H_m}=\begin{bmatrix}\tilde{u}_{m,i}^{\mathcal{H}}(0)\\ \vdots\\ \tilde{u}_{m,i}^{\mathcal{H}}(J-1)\end{bmatrix}^T\begin{bmatrix}H_m(\exp(j\frac{2\pi}{N}l_{m,0}))& & \\ & \ddots & \\ & & H_m(\exp(j\frac{2\pi}{N}l_{m,J-1}))\end{bmatrix}=\begin{bmatrix}H_m(\exp(j\frac{2\pi}{N}l_{m,0}))\\ \vdots\\ H_m(\exp(j\frac{2\pi}{N}l_{m,J-1}))\end{bmatrix}^T\begin{bmatrix}\tilde{u}_{m,i}^{\mathcal{H}}(0)& & \\ & \ddots & \\ & & \tilde{u}_{m,i}^{\mathcal{H}}(J-1)\end{bmatrix}. \tag{8}$$

$$\tilde{\mathbf{u}}_{m,i}^{\mathcal{H}}\mathbf{D}_{H_m}=\underbrace{\begin{bmatrix}h_m(0)\\ \vdots\\ h_m(L)\end{bmatrix}^T}_{\mathbf{h}_m^T}\underbrace{\begin{bmatrix}1 & \cdots & 1\\ \exp(-j\frac{2\pi}{N}l_{m,0}) & \cdots & \exp(-j\frac{2\pi}{N}l_{m,J-1})\\ \vdots & \cdots & \vdots\\ \exp(-jL\frac{2\pi}{N}l_{m,0}) & \cdots & \exp(-jL\frac{2\pi}{N}l_{m,J-1})\end{bmatrix}}_{\mathbf{A}_m}\underbrace{\begin{bmatrix}\tilde{u}_{m,i}^{\mathcal{H}}(0)& & \\ & \ddots & \\ & & \tilde{u}_{m,i}^{\mathcal{H}}(J-1)\end{bmatrix}}_{\mathbf{D}_{u_{m,i}}}. \tag{9}$$

channel estimation, linear and DF receivers, and the merits of precoding versus channel coding. For GMC-CDMA with BPSK constellation and a linear ZF-receiver the average BER is [7]:

$$P(e)=\frac{1}{2MK}\sum_{m=0}^{M_a-1}\sum_{k=0}^{K-1}\text{erfc}\Big(\sqrt{\frac{1}{\bar{\boldsymbol{\gamma}}_{m,k}^{\mathcal{H}}\bar{\boldsymbol{\gamma}}_{m,k}\epsilon_{m,k}}\frac{E_b}{N_0}}\Big), \tag{11}$$

where $\bar{\boldsymbol{\gamma}}_{m,k}^{\mathcal{H}}$ is the kth row of the matrix $\boldsymbol{\Gamma}_m\mathbf{G}_m$, $\epsilon_{m,k}:=\sum_{i=0}^{P-1}|c_{m,k}(i)|^2$ is the energy of the mth user's kth code, and E_b/N_0 is the bit SNR. For our GMC-CDMA system we always choose the precoder $\mathbf{F}_m$ as in (3). In all following examples, we average the BER performance for 100 random channel realizations (Rayleigh fading).

Case 1: Different inner-spreadings $\boldsymbol{\Theta}_m$

In Fig. 3 we plot (11) for an GMC-CDMA system with WH-S, PN-S, and Va-S. The maximum number of users is $M=16$, each one transmitting blocks of symbols drawn from a BPSK constellation. The length of the $\mathbf{s}_m(i)$ blocks is $K=8$. The transmitted signal propagates through a Rayleigh fading channel of order $L=3$ which is assumed to be known at the receiver. We decrease the number of active users in the system from $M_a=16$ down to 2 and each time we increase the amount of bandwidth allocated per user by increasing J. To maintain guarantees on symbol recovery we replace the WH-S code matrix $\boldsymbol{\Theta}_m$ with a PN-S matrix when the number of active users is larger then $M_a=10$. The theoretical BER curves from Fig. 3 show that under different load conditions there is practically no difference in performance when the Va-S is used. Nevertheless, the Va-S performs better in full load than PN-S or WH-S. When the load decreases (under 65% in this example) a WH-S code matrix $\boldsymbol{\Theta}_m$ improves performance.

Case 2: Performance of blind channel estimation

Performance of the GMC-CDMA blind channel estimation algorithm is assessed by simulating a system that uses an inner-code matrix $\boldsymbol{\Theta}_m$ with equiprobable ±1, $\pm j$ entries, designed for $K=10$, $L=5$, and $M=8$ users. A linear ZF receiver is used to estimate the transmitted symbols. The number of active users in the system is selected to be $M_a\in\{2,5,8\}$. We process $N_b=30$ blocks, each block having size P. The average BER of our blind GMC-CDMA system is plotted in Fig. 4 along with the theoretical BER curves obtained from (11). From Fig. 4 we infer that GMC-CDMA is able to identify and estimate the channel reliably even at low SNR.

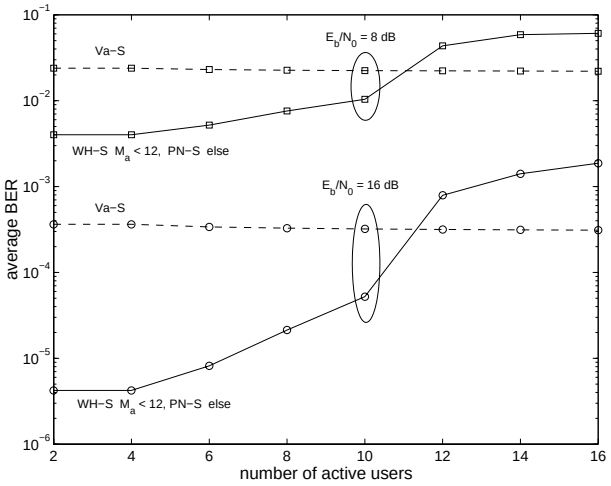

Figure 3: GMC-CDMA with different number of active users: $M=16$, $K=8$, $L=3$

Case 3: Comparison of linear and DF receivers

Next, for a GMC-CDMA system with $M=16$, $K=10$, and $L=5$ we compare the ZF-DF and the linear ZF receivers for a different number of active users (i.e., $M_a\in\{2,8,16\}$). The average BER of the linear ZF receiver is determined using (11) whereas the performance of the ZF-DF receiver is assessed by simulations. We assume perfect CSI at the receiver end. It can be deduced from Fig. 5 that the ZF-DF receiver results in improved BER compared to its linear counterpart. To study the performance of our multiuser DF receiver, we look at a GMC-CDMA system with $M=16$, $K=8$, $L=3$, which uses either WH or Va-

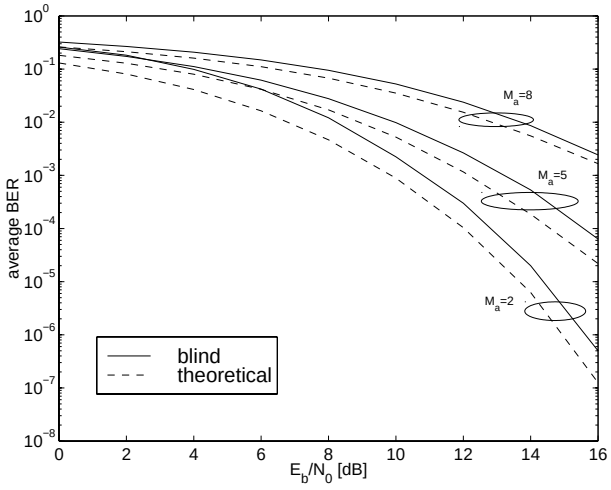

Figure 4: Blind GMC-CDMA with random codes and ZF receiver for $M = M_a = 8$, $K = 10$, $L = 5$, $I = 30$

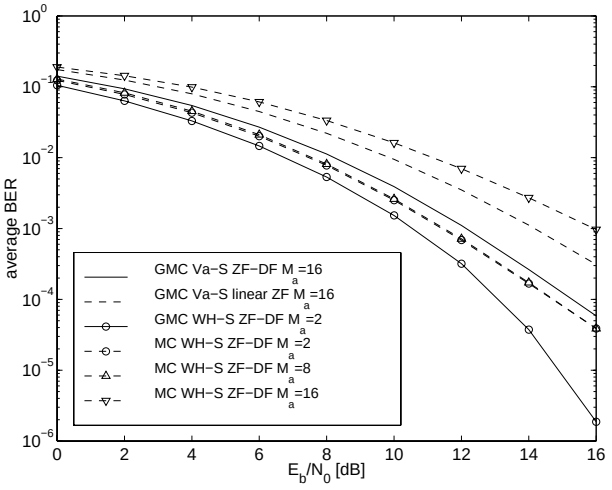

Figure 6: GMC-CDMA with $K = 8$ *v.* MC-CDMA with $P = 19$: ZF-DF, $M = 16$, $L = 3$

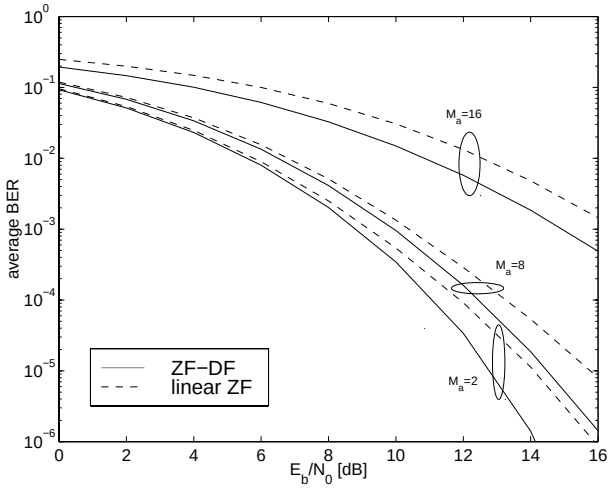

Figure 5: GMC-CDMA PN-S with $M = 16$, $K = 10$, $L = 5$: linear-ZF *v.* ZF-DFE

S codes for $\mathbf{\Theta}_m$. In Fig. 6 we compare the BER of our GMC-CDMA system with MC-CDMA using WH codes with spreading $P = 19$ for variable number of active users. We deduce from the figure that GMC-CDMA outperforms MC-CDMA for the same number of active users. Moreover, GMC-CDMA with $M_a = M = 16$ (full load) using Va-S is close in performance to MC-CDMA with $M_a = 8$ (half load).

Case 5: Precoding *v.* Channel Coding

Instead of precoding the K symbols through the matrix $\mathbf{\Theta}$ to produce J symbols, we could alternatively introduce redundancy via error-correction coding (we call this "coding method" for short). In this example, we will compare the BER performance of our precoding method with coding method. In Fig. 7, we simulate a system with $K = 11$, $L = 4$, and $M = 16$. We use the Va-S for our linear precoding. For the coding method, we use BCH codes with generating polynomial $D^4 + D^3 + 1$ to encode the 11 symbols, and the resulting length-15 codeword is put on the $J = K + L = 15$ subcarriers. The channels consist of 5 equal variance complex Gaussian taps and 100 random channel realizations are used to average the channel-dependent performance. At the receiver, the performance of linear zero-forcing equalization for precoding is compared with that of hard-decision based MLSE for the coding method. The low-complexity linear equalizer in precoding outperforms the coding method, part of the reason being the fact that hard-decision is used before the (higher complexity) MLSE is used in the coding method. To distinguish the major factor affecting the performance, BER's of soft-decision based MLSE for both precoding and coding methods are also reported in the same figure. As we can see, the precoding method again outperforms the coding method. The main reason is that precoding directly combats frequency selective fading and thus avoids symbol recovery problems, while the coding method relies on general-purpose codes to correct (persistent) errors caused by channel null(s) on or close to users' subcarriers. Of course, combining coding and precoding should lead to even better performance at the expense of reducing system bandwidth efficiency as more redundancy is needed. The reader is reminded that in the coding method, we encode the information symbol blocks (of size K) separately. Coding over many blocks combined with interleaving could improve BER performance but would also incur longer decoding delay than the single block precoding framework dealt with in this paper.

Case 6: Comparison of GMC-CDMA to SS-MC-MA

In order to emphasize how important it is for a system to offer guarantees on symbol recovery we compare the performance of the coded GMC-CDMA with $K = 36$ to the performance of an equivalent Spread-Spectrum Multicarrier Multiple-Access (SS-MC-MA) system with $K = 4$ pro-

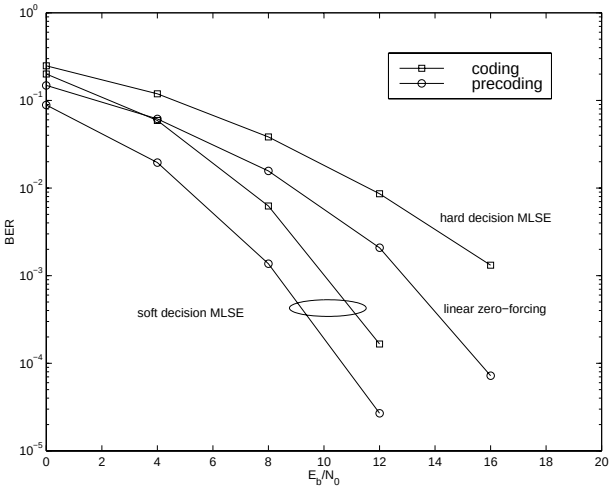

Figure 7: Precoding *v.* Block Channel Coding

posed in [10]. Out of $M = 8$ possible users, only $M_a = 5$ users are active and the block-size K is selected such that the two systems have the same bandwidth efficiency. Both systems use a rate 1/2 convolutional encoder with memory 6 (133,171). A linear-ZF receiver supplies the metrics to the soft-decision Viterbi decoder. We consider a channel with $L + 1 = 4$ taps (generated as i.i.d. complex Gaussian variables). We average the BER over 100 channel realizations, and Fig. 8 illustrates the resulting BERs. As SS-MC-MA cannot guarantee symbol recovery, its performance is inferior to that of GMC-CDMA: at around 10dB, which is a nominal operating range for wireless systems, the gap in BER is almost an order of magnitude.

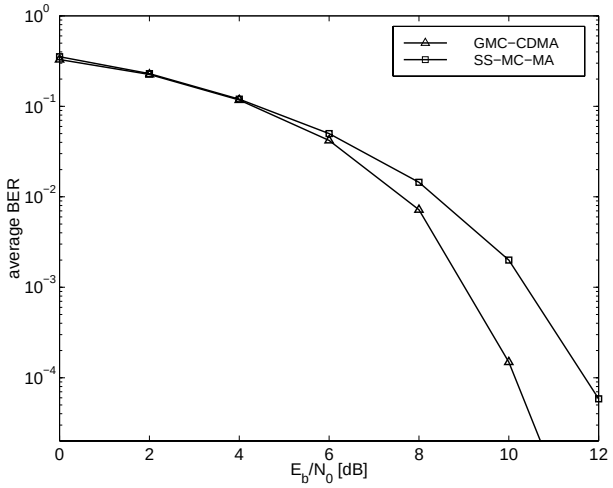

Figure 8: Precoding *v.* Convolutional Channel Coding

9 CONCLUSIONS

In this work we have developed an all-digital GMC-CDMA framework capable of modeling existing multiuser multicarrier spread-spectrum systems. Using our framework, we identified fundamental shortcomings of existing systems, which are unable to guarantee MUI suppression and symbol recovery without undue sacrifices in terms of bandwidth or implementation complexity. Addressing the need for increased BER performance (which is a must for provision of Quality of Service in emerging wireless networks), herein we outlined a reception/transmission scheme, which, while requiring small FFT-based implementation overhead, guarantees MUI elimination and symbol recovery regardless of the physical FIR channel. Based on an inner-code/outer-code design procedure, our scheme is versatile enough to exploit situations of reduced load in the system, and utilize non-linear (DF) receivers. The data transmission rate can be further increased by taking advantage of our blind channel estimation algorithm which dispenses with training sequences, and through simulations we illustrated that our system results in improved BER performance. Further BER improvements can be achieved by exploiting space-time block-coded transmissions (see [12, 18] for preliminary results), and optimizing our system either in the deterministic sense (when the channel is known to the transmitter) or in the stochastic sense (when only statistical description of the fading channels is available at the transmitter).

ACKNOWLEDGEMENT

The work in this paper has been supported by NSF CCR Grant No. 98-05350, and NSF Wireless Initiative Grant No. 99-79443.

REFERENCES

[1] Q. Chen, E. S. Sousa, and S. Pasupathy. Performance of a coded multi-carrier DS-CDMA system in multipath fading channels. *Wireless Personal Communications*, 2:167–183, 1995.

[2] V. M. DaSilva and E. S. Sousa. Multicarrier orthogonal CDMA signals for quasi-synchronous communication systems. *IEEE Journal on Selected Areas in Communications*, pages 842–852, June 1994.

[3] S.N. Diggavi. Multiuser DMT: a multiple access modulation scheme. In *Proc. of GLOBECOM*, pages 1566–1570, New York, NY, 1996.

[4] K. Fazel. Performance of CDMA/OFDM for mobile communication system. In *Proceedings of 2nd IEEE International Conference on Universal Personal Communications*, pages 975–9, Ottawa, Ont., Canada, 1993.

[5] K. Fazel and G. P. Fettweis (Eds). *Multi-Carrier Spread Spectrum*. Kluwer Academic Publishers, 1997.

[6] G. B. Giannakis, P. A. Anghel, and Z. Wang. All-Digital Unification and Equalization of Generalized Multi-Carrier CDMA through Frequency-Selective Uplink Channels. *IEEE Trans. on Communications*, March 2000 (submitted).

[7] G. B. Giannakis, Z. Wang, A. Scaglione, and S. Barbarossa. AMOUR — Generalized Multicarrier Transceivers for Blind CDMA regardless of Multipath. *IEEE Trans. on Communications*, 2000 (to appear).

[8] J.C. Haartsen. The Bluetooth radio system. *IEEE Personal Communications*, 7:28–36, February 2000.

[9] S. Hara and R. Prasad. Overview of Multicarrier CDMA. *IEEE Communications Magazine*, pages 126–133, December 1997.

[10] S. Kaiser and K. Fazel. A spread spectrum multi-carrier multiple access system for mobile communications. In *First Workshop on Multi-Carrier Spread-Spectrum*, pages 49–56, Oberpfaffenhofen, Germany, 1997.

[11] S. Kondo and L. B. Milstein. Performance of multicarrier DS CDMA systems. *IEEE Trans. on Communications*, 44(2):238–46, February 1996.

[12] Z. Liu and G.B. Giannakis. Space-Time Block Coding with Transmit Antennas for Multiple Access Irrespective of Multipath. *IEEE Trans. on Communications*, 1999 (submitted). See also *Proc. of the 1st Sensor Array and Multichannel SP Workshop*, Boston, MA, May 15-17, 2000.

[13] Van Nee and R. Prasad. *OFDM for Wireless Multimedia Communications*. Artech House, 2000.

[14] D.N. Rowitch and L.B. Milstein. Convolutionally Coded Multicarrier DS-CDMA Systems in a Multipath Fading Channel — Part I: Performance Analysis. *IEEE Trans. on Communications*, 47(10):1570–1582, October 1999.

[15] A. Scaglione, G. B. Giannakis, and S. Barbarossa. Redundant filterbank precoders and equalizers, Part I: Unification and optimal designs. *IEEE Trans. on Signal Processing*, 47(7):1988–2006, July 1999.

[16] E. Sourour and M. Nakagawa. Performance of Orthogonal Multicarrier CDMA in a multipath fading channel. *IEEE Trans. on Communications*, 44(3):356–67, March 1996.

[17] A. Stamoulis and G. B. Giannakis. Packet Fair Queueing Scheduling Based on Multirate Multipath-Transparent CDMA for Wireless Networks. In *Proc. of INFOCOM2000*, pages 1067–1076, Tel Aviv, Israel, March 2000.

[18] A. Stamoulis and G.B. Giannakis. Supporting Integrated Services in Wireless Networks with Space-Time Block-Coded Transmissions. In *Proc. 34th Annual Asilomar Conference on Signals, Systems and Computers*, Pacific Grove, California, November 2000.

[19] A. Stamoulis, G.B. Giannakis, and A. Scaglione. Block FIR Decision-Feedback Equalizers for Filterbank Precoded Transmissions with Blind Channel Estimation Capabilities. *IEEE Trans. on Communications*, 2000 (to appear).

[20] L. Vandendorpe. Multitone spread spectrum multiple access communications systems in a multipath Rician fading channel. *IEEE Trans. on Vehicular Technology*, 44:327–337, May 1995.

[21] S. Verdú. *Multiuser Detection*. Cambridge University Press, 1998.

[22] Z. Wang and G. B. Giannakis. Block spreading for multipath-resilient generalized multi-carrier CDMA. In G. B. Giannakis, Y. Hua, P. Stoica, and L. Tong, editors, *Signal Processing Advances in Wireless Communications*, volume II. Prentice-Hall, Inc, 2000 (to appear).

[23] Z. Wang and G.B. Giannakis. Block Precoding for MUI/ISI-Resilient Generalized Multi-carrier CDMA with Multirate Capabilities. In *Proc. of Intl. Conf. on Communications*, New Orleans, LA, June 18-22, 2000.

[24] Z. Wang and G.B. Giannakis. Wireless Multicarrier Communications: Where Fourier Meets Shannon. *IEEE Signal Processing Magazine*, 17(3):29–48, May 2000.

[25] N. Yee, J-PMG. Linnartz, and G. Fettweis. Multi-carrier CDMA in indoor wireless radio networks. *IEICE Transactions on Communications*, E77-B(7):900–904, July 1994.

[26] S. Zhou, G.B. Giannakis, and A. Swami. Frequency-Hopped Generalized Multicarrier CDMA for Multipath and Interference Suppression. In *MILCOM 2000 Proceedings*, Los Angeles, CA, USA, October 2000 (to appear).